DOI: 10.1002/ejic.200800665

A 2D Layered Metal–Organic Framework Constructed by Using a Hexanuclear Manganese Metallamacrocycle as a Supramolecular Building Block

Jeungwook Choi,[a] Jaejoon Park,[a] Mira Park,[a] Dohyun Moon,[a] and Myoung Soo Lah*[a]

Keywords: Metallacycles / Macrocycles / Supramolecular chemistry / Metal–organic frameworks / Layered compounds

The hexanuclear manganese metallamacrocycle $[Mn_6(Haahz)_6(dmso)_6]$ (**1**) was prepared by using a new pentadentate ligand, *N*-acetylaminobenzhydrazide (H_4aahz), and a manganese ion as primary building blocks in dimethyl sulfoxide (dmso). Under identical conditions but in the presence of 1,2-bis(4-pyridyl)ethane (bpea) as an *exo*-bidentate linker in dimethylformamide (dmf), the 2D layered metal–organic framework (MOF) $[Mn_6(Haahz)_6(bpea)_2(dmf)_2]_n$ (**2**) was obtained, where the hexanuclear manganese metallamacrocycle served as a supramolecular building block. The network topology of **2**, a 3-connected 4.8^2 topology, is quite different from those of the MOFs obtained from a similar pentadentate ligand, *N*-acylsalicylhydrazide, although the same hexanuclear manganese metallamacrocycles were used as supramolecular building blocks and bpea was used as the same linker ligand. Although the layers of **2** are staggered relative to each other, the network has quite a large solvent cavity between the layers, because of the corrugated nature of the layer.

Introduction

Metal–organic frameworks (MOFs) have attracted the attention of researchers, because of their potential in various applications such as gas storage, separation, and catalysis.[1] However, rational design of MOFs is still a difficult task, because a small change in the primary building blocks often leads to an MOF of completely different architecture. The strategy of using secondary building units (SBUs) has provided a better opportunity for rational design.[2] Secondary building units that are constructed from a series of primary building units can afford various isostructural architectures with variable porosities and functionalities, depending on the primary building units used.[3] The supramolecular building block (SBB) approach is another effective way to construct various MOFs,[4] and the structures and properties of the final MOFs can be controlled or modulated at a more predictable supramolecular building block level rather than at the less predictable primary building block level.[4h]

Hexanuclear manganese metallamacrocycles have been prepared by treating a series of pentadentate *N*-acylsalicylhydrazide ligands with manganese(II) acetate tetrahydrate.[5] Because each distorted octahedral metal center in the hexanuclear manganese metallamacrocycle has been coordinated by five donor atoms from two chelating pentadentate ligands, the one replaceable solvent site left can be utilized as a nodal point in framework construction. Hence, these potential hexatopic metallamacrocycles were used as SBBs for the construction of three-dimensional (3D) network structures, where the metallamacrocycles have served either as rectangular tetratopic or octahedral hexatopic nodes.[6]

We synthesized the new pentadentate ligand *N*-acetylaminobenzhydrazide (H_4aahz). The hydroxy group of the phenoxy residue of an *N*-acylsalicylhydrazide was replaced by an amino group (Scheme 1), where the *N*-acylsalicylhydrazide is well established as a primary building unit for a metallamacrocyclic architecture.[7] We investigated a substi-

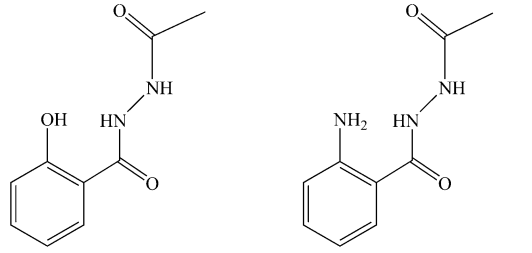

N-acetylsalicylhydrazide (H_3ashz) — *N*-acetylaminobenzhydrazide (H_4aahz)

Scheme 1. Two similar potential pentadentate ligands, one with a hydroxy group and the other with an amino group.

[a] Department of Chemistry and Applied Chemistry, College of Science and Technology, Hanyang University,
1271 Sa-1-dong, Ansan, Kyunggi-do 426-791, Korea
Fax: +82-31-436-8100
E-mail: mslah@hanyang.ac.kr

Supporting information for this article is available on the WWW under http://www.eurjic.org or from the author.

tution effect in a primary building unit on the formation of the metallamacrocycle and on the subsequent self-assembly of a MOF based on the metallamacrocycle as an SBB.

Results and Discussion

The new pentadentate ligand, H_4aahz, was prepared by using a similar method to that used in the preparation of *N*-acetylsalicylhydrazide (H_4ashz), which involved coupling equivalent amounts of aminobenzhydrazide with acetic anhydride in the presence of triethylamine as a base in chloroform. A hexanuclear manganese metallamacrocycle can be synthesized by using H_4aahz and manganese ions as primary building units in dmso solution (Scheme 2).

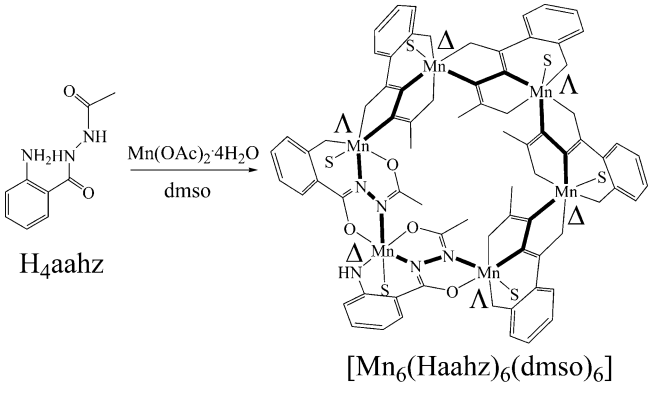

Scheme 2. A hexanuclear manganese metallamacrocyle is self-assembled from six H_4aahz ligands in a trianionic Haahz^{3-} form, six manganese ion, and six solvent dmso molecules.

The hexanuclear manganese metallamacrocycle [Mn_6(Haahz)$_6$(dmso)$_6$] (**1**) (Figure 1) is very similar to the reported hexanuclear manganese metallamacrocycle [Mn_6(ashz)$_6$(dmf)$_6$] obtained by using the H_3ashz ligand, which has a hydroxy phenyl residue.[5b]

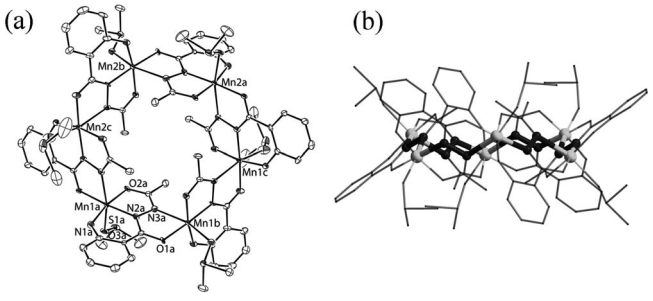

Figure 1. (a) An ORTEP diagram of hexanuclear manganese metallamacrocycle **1**; (b) side view of **1** in a line drawing, where the atoms and the bonds in the 18-membered macrocyclic ring are highlighted in a ball-and-stick drawing.

Although the ligand can serve as either a dianionic or trianionic pentadentate ligand depending on the deprotonation status of the amino group, the ligand is in a trianionic state in the cluster. The deprotonation status of the amino group is dependent on the pK_a of the amino group, which is influenced by the metal ion used and the solvent molecules involved.[8] In **1**, the amino group of the ligand is singly deprotonated, and the ligand is in a trianionic state. The bond between the carbon atom of the aromatic phenyl ring and the nitrogen atom of the amino group in the nondeprotonated state has C–N single-bond character,[8,9] whereas the corresponding bond in the singly deprotonated state has double-bond character (see Table 1).[10]

Table 1. Selected bond lengths (Å) for **1** and **2**.

	1	2		1	2
Mn1–O1C[a]	1.981(4)	1.977(1)	Mn1–O2A	1.949(4)	1.955(1)
Mn1–N1A	1.916(6)	1.908(2)	Mn1–N2A	1.958(6)	1.961(2)
Mn1–N3C[a]	2.248(6)	2.255(2)	Mn1–O3A	2.313(5)	2.333(2)
Mn2–O1A	1.973(4)	1.965(1)	Mn2–O2B	1.960(5)	1.944(1)
Mn2–N1B	1.900(6)	1.909(2)	Mn2–N2B	1.957(5)	1.952(2)
Mn2–N3A	2.292(6)	2.266(2)	Mn2–O3B	2.236(5)	2.323(2)
Mn3–O1B	1.973(5)	1.992(1)	Mn3–O2C	1.966(5)	1.950(1)
Mn3–N1C	1.898(5)	1.898(2)	Mn3–N2C	1.968(5)	1.963(2)
Mn3–N3B	2.267(6)	2.263(2)	Mn3–O3C	2.256(6)	2.335(2)
N1A–C1A	1.376(9)	1.359(3)	N1B–C1B	1.354(10)	1.353(3)
N1C–C1C	1.346(9)	1.353(2)			

[a] Symmetry code: $-x + 1, -y, -z$ for **1**; $-x + 1, -y + 2, -z$ for **2**.

The triply deprotonated ligand Haahz^{3-} was able to bridge the metal ions by using a hydrazide N–N group. The *N*-methyl groups of the ligands are directed towards the inner side of the macrocyclic ring, and the phenyl residues are directed towards the outer side of the macrocyclic ring (Figure 1a). The Haahz^{3-} ligand serves as a pentadentate ligand and each manganese(III) center is in a Jahn–Teller distorted octahedral geometry (Table 1) with tridentate–bidentate chelation modes from two Haahz^{3-} ligands, and an additional solvent molecule is ligated in an axial position. Three solvent molecules coordinated at the alternating metal centers in **1** are on one face of the complex, and the other three solvent molecules coordinated at the remaining metal centers are on the other face of the complex.

The tridentate–bidentate binding mode of the ligand around the metal center forces the stereochemistry of the metal ion into a propeller configuration in hexanuclear manganese metallamacrocycle **1**. The chiralities of the metal centers in the metallamacrocycle alternate between Δ and Λ forms (Figure 2), and this alternation leads to the hexanuclear manganese metallamacrocycle having two faces with opposite chiralities. The metal ions in hexanuclear metallamacrocycle **1** are in a –$(\Delta\Lambda)_n$– chiral sequence, as in the corresponding ashz analogue, the hexanuclear manganese metallamacrocycle [Mn_6(ashz)$_6$(dmf)$_6$].

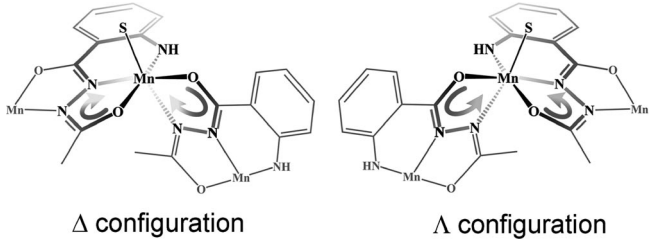

Figure 2. Schematic diagram for Δ/Λ chiral configurations around the metal center of the propeller bidentate–tridentate binding mode observed in **1**.

The 2D layered MOF $[Mn_6(Haahz)_6(dmf)_2(bpea)_2]$ (**2**) was prepared under identical reaction conditions except for the presence of the *exo*-bidentate linker bpea in dmf solvent, where only four of the six solvent sites in the hexanuclear manganese metallamacrocyclic building block were substituted by the bpea ditopic linker (Figure 3 and Figure S1 in the Supporting Information).

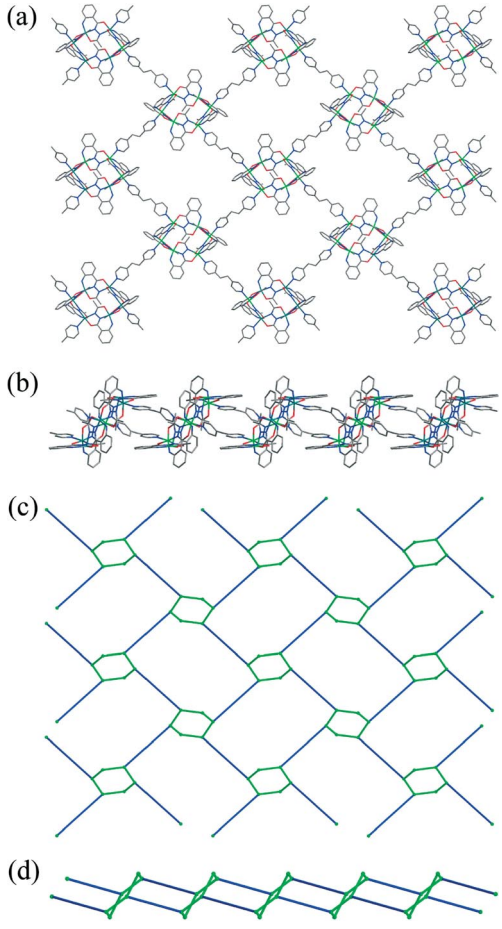

Figure 3. (a) Top view of a layer of 2D network **2**; (b) side view of the layer of network **2**; (c) metallamacrocycles in network **2** were simplified as green hexagons and bpea linkers as blue sticks; (d) simplified side view of the layer.

The hexanuclear manganese metallamacrocycle served as an SBB and the bpea served to interconnect the building blocks for the formation of 2D layered MOF **2**. The MOF has a 3-connected 4.8^2 network topology (Figure 3c).[11] When the SBB was reduced to a planar rectangular 4-connected node, the net could be further simplified to a 4-connected 4^4 net. Framework **2** has a completely different network topology from that of the MOFs containing *N*-acylsalicylhydrazide as the primary building unit. Although the hexanuclear metallamacrocycle is similarly used as an SBB and the same bpea linker is used for substitution, the MOFs have 3D network topologies.[6d] The 2D sheets in network **2** are staggered relative to each other (Figure 4a,b and Figure S2a in the Supporting Information). However, the network has quite a large solvent cavity, because of the corrugated nature of the 2D sheet (Figure 3c,d, Figure 4c,d, and Figure S2b in the Supporting Information). The cavity volume of network **2** was estimated by the PLATON program[12] to be about 5000 $Å^3$ per unit cell, which corresponds to about 40% of the unit cell volume.

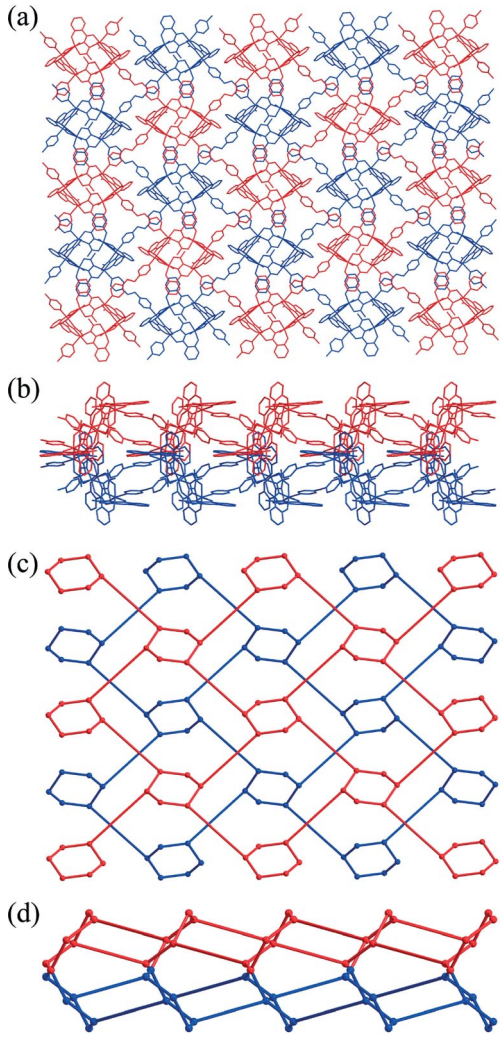

Figure 4. Line drawing of two layers of 2D network **2** showing the staggering of the layers. The two staggered layers are differentiated by using red and blue: (a) top view; (b) side view; (c) schematic top view; (d) schematic side view.

Thermogravimetric analysis (TGA) of network **2** shows a weight loss of about 28.8% below 190 °C, which corresponds to the loss of water and dmf molecules as structural solvents (calcd. 28.3% for nine dmf molecules and seven H_2O molecules; Figure 5). The decomposition temperature for the network was observed to be approximately 320 °C. This result agrees with the elemental analysis result and suggests that the water molecules from air are probably absorbed on the surface of the framework.

The powder X-ray diffraction (PXRD) pattern of the ground bulk crystalline sample of network **2** is slightly different from the simulation from the structure of a single-crystal X-ray diffraction study (Figure 6). Considering the homogeneity of the bulk crystals observed by optical microscopy, the observation of identical unit cell parameters for

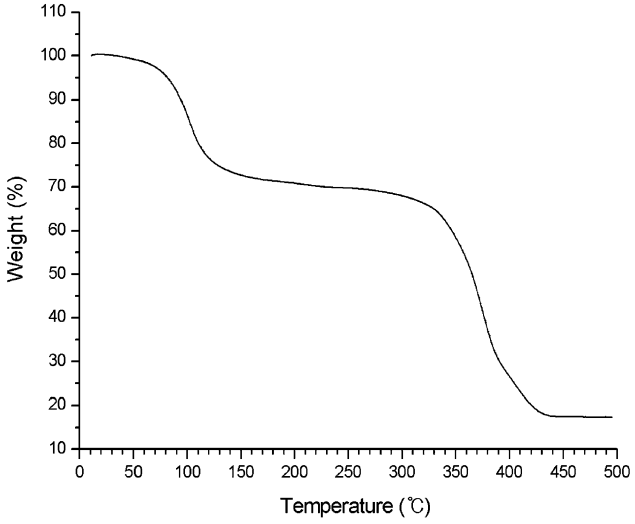

Figure 5. TGA of network **2**.

several single crystals coated with paratone oil at low temperature, and the partial matches in the peak positions of the PXRD of the unground bulk crystalline sample of network **2** with the simulated PXRD, we believe that the single crystal represents the bulk sample. The difference in the PXRD patterns suggests that the ground bulk crystalline sample of network **2** loses some of its solvent from the cavity, which causes the deformation of network **2** to an unidentified structure. However, the amorphous pattern of the activated sample prepared by soaking the network in dichloromethane for 5 h and vacuum drying it at ambient temperature suggests that the network has completely collapsed when all of the solvent in the cavity is removed. Not surprisingly, the N_2 sorption isotherm of the activated network is a type II isotherm, which is typical for a nonporous material.

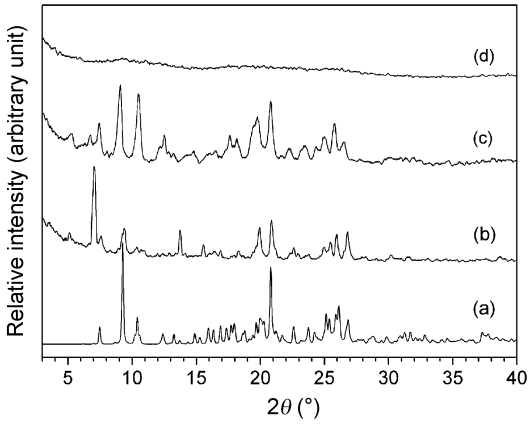

Figure 6. PXRD patterns of network **2**: (a) simulated PXRD from a single-crystal structure of network **2**; (b) PXRD of as-synthesized unground network **2**; (c) PXRD of as-synthesized network **2** ground to a fine powder; (d) PXRD of an activated sample prepared by soaking network **2** in dichloromethane for 5 h and vacuum drying at ambient temperature.

Conclusions

We synthesized neutral hexanuclear manganese metallamacrocycle **1** by using H_4aahz as a new type of pentadentate ligand, where the hydroxy group of H_3ashz is replaced by an amino group. Although it is possible for H_4aahz to be in a dianionic H_2aahz^{2-} form depending on the metal ion involved, the ligand is in a trianionic pentadentate $Haahz^{3-}$ form in **1**. The metal centers in **1** have alternating Δ and Λ configurations, and this alternation leads to a macrocyclic system of S_6 symmetry. Metallamacrocycle **1** can be utilized as an SBB for the construction of 2D layered framework **2**, where four of the six replaceable solvent sites are substituted by the *exo*-bidentate ligand bpea. Even though a similar hexanuclear metallamacrocycle is used as an SBB and the method of substitution is similar, the network topology of resulting MOF **2** is quite different from those of the reported 3D MOFs. MOF **2** has a 3-connected 4.8^2 network topology and can be further simplified to a 4-connected 4^4 net when the SBB is treated as a rectangular tetranode. Although the layers in the 2D layered network are staggered, the network has a large solvent cavity between the layers because of their corrugated nature.

Experimental Section

Materials and Instrumentations: The following materials were used as received with no further purification: 1,2-bis(4-pyridyl)ethane (bpea), aminobenzhydrazide, acetic anhydride, and triethylamine from Aldrich, Inc.; manganese(II) acetate tetrahydrate from Yakuri; dimethyl sulfoxide (dmso), *N*,*N*-dimethylformamide (dmf), and chloroform from Junsei Chemical Co., Ltd.

Instrumentation: Elemental analyses (C, H, and N) were performed at Sogang University. Infrared spectra were recorded in the range 4000–400 cm^{-1} with a BioRad FTS-6000 spectrometer. ^1H and ^{13}C NMR spectra were obtained by using a Varian-300 spectrometer (^1H at 300 MHz and ^{13}C at 75 MHz). TGA was performed by using a SCINCO STA S-1000 in air.

***N*-Acetylaminobenzhydrazide (H_4aahz):** To a solution of aminobenzhydrazide (0.453 g, 3.00 mmol) dissolved in chloroform (70 mL) cooled in an ice bath was slowly added acetic anhydride (0.283 mL, 3.00 mmol), followed by the slow addition of triethylamine (0.418 mL, 3.00 mmol), and the mixture was heated at reflux for 1 d. A white precipitate was obtained, which was washed with cold chloroform, water, and ether, and the residue was then dried in a freeze drier. Yield: 0.438 g (75.6%). M.p. 185–187 °C. ^1H NMR ([D_6]dmso): δ = 9.95 (br. s, 1 H, N*H*), 9.76 (br. s, 1 H, N*H*), 7.52 (d, 1 H, Ar*H*), 7.19 (t, 1 H, Ar*H*), 6.71 (d, 1 H, Ar*H*), 6.53 (t, 1 H, Ar*H*), 6.40 (br. s, 2 H, NH_2), 1.91 (s, 3 H, CH_3) ppm. ^{13}C NMR ([D_6]dmso): δ = 168.8, 168.1, 150.0, 132.4, 128.2, 116.5, 114.7, 112.5, 20.7 ppm. IR (ATR): $\tilde{\nu}$ = 3471 (s), 3353 (s), 3261 (s), 3200 (s), 3019 (s), 2162 (s), 1980 (s), 1685 (m), 1638 (s), 1588 (w), 1541 (m), 1513 (s), 1492 (s), 1429 (m), 1372 (w), 1289 (m), 1251 (s), 1163 (m), 1036 (w), 1005 (w), 900 (m), 763 (s) cm^{-1}. $C_9H_{11}N_3O_2$ (193.20): calcd. C 55.95, H 5.74, N 21.75; found C 55.83, H 5.67, N 21.75.

$[Mn_6(Haahz)_6(dmso)_6]$ (1): To a solution of H_4aahz (0.0579 g, 0.300 mmol) dissolved in dmso (20 mL) was added manganese(II) acetate tetrahydrate (0.0735 g, 0.300 mmol), and the solution was left to stand in a capped vial. Dark brown crystals were obtained

after 30 d. The crystals were filtered through a frit and vacuum dried at ambient temperature. Yield: 0.0638 g (65.8%). IR (ATR): $\tilde{\nu}$ = 3402 (s), 3250 (s), 2952 (s), 2865 (m), 2162 (w), 1689 (m), 1644 (m), 1608 (m), 1600 (m), 1492 (s), 1448 (m), 1390 (w), 1310 (s), 1230 (s), 1160 (w), 1140 (w), 1033 (m), 1006 (m), 955 (w), 901 (m), 742 (s) cm^{-1}. $Mn_6C_{66}H_{96}N_{18}O_{18}S_6$ (1951.58): calcd. C 40.62, H 4.96, N 12.92; found C 41.10, H 4.57, N 13.34.

$[Mn_6(Haahz)_6(dmf)_2(bpea)_2]$ (2): To a solution of H_4aahz (0.0193 g, 0.100 mmol) dissolved in dmf (20 mL) was added bpea (0.0184 g, 0.100 mmol), followed by the addition of manganese(II) acetate tetrahydrate (0.0245 g, 0.100 mmol), and the solution was left to stand in a capped vial. Dark brown crystals were obtained after 30 d. The crystals were filtered through a frit and air dried at ambient temperature. Yield: 0.0344 g (73.0%). IR (ATR): $\tilde{\nu}$ = 3404 (s), 3251 (s), 2950 (s), 2864 (m), 1684 (w), 1650 (s), 1601 (s), 1560 (s), 1496 (s), 1448 (w), 1379 (s), 1336 (s), 1253 (s), 1154 (w), 1095 (m), 1063 (w), 1033 (w), 979 (w), 955 (w), 900 (m), 856 (w), 815 (w), 781 (w), 747 (m), 699 (m), 662 (w) cm^{-1}. $Mn_6C_{111}H_{163}N_{33}O_{30}$ {$[Mn_6(Haahz)_6(dmf)_2(bpea)_2]$·9dmf·7$H_2O$, 2769.34}: calcd. C 48.14, H 5.93, N 16.69; found C 47.65, H 5.60, N 17.13.

Crystallographic Data Collection and Refinement of Structures: A crystal of **1** was coated with paratone oil to prevent loss of crystallinity on exposure to air. The data collection was performed at 173 K with Mo-K_α radiation (λ = 0.71073 Å) with a Bruker SMART CCD equipped with a graphite crystal, incident-beam monochromator. The SMART and SAINT software packages[13] were used for data collection and integration, respectively. The collected data were corrected for absorption by using SADABS[14] based upon Laue symmetry by using equivalent reflections. A crystal of **2** was also coated with paratone oil, because the crystal loses its crystallinity on exposure to air. The diffraction data were measured at 100 K with synchrotron radiation (λ = 0.70000 Å) with a 4AMXW ADSC Quantum-210 detector with a Pt-coated Si double crystal monochromator at the Pohang Accelerator Laboratory, Korea. The ADSC Quantum-210 ADX program[15] was used for data collection, and HKL2000 (ver. 0.98.698a)[16] was used for cell refinement, reduction, and absorption correction.

Crystal Data for $[Mn_6(Haahz)_6(dmso)_6]$·12dmso (1): $Mn_6C_{90}H_{156}N_{18}O_{30}S_{18}$, fw = 2877.05 g mol^{-1}, triclinic, space group $P\bar{1}$, a = 13.180(4) Å, b = 14.804(4) Å, c = 17.739(5) Å, α = 70.997(4)°, β = 86.675(5)°, γ = 78.248(5)°, V = 3203.7(15) Å^3, Z = 1, μ(Mo-K_α, λ = 0.71073 Å) = 0.941 mm^{-1}, 15166 reflections were collected, 10770 were unique (R_{int} = 0.0404). The structure was solved by a direct method and refined by full-matrix least-squares calculations with the SHELXTL-PLUS software package.[17] Three manganese atoms, three ligand units, three coordinating dmso molecules, and six noncoordinating dmso sites were identified as the asymmetric unit. All non-hydrogen atoms except some of the disordered dmso molecules were refined anisotropically; all hydrogen atoms were assigned isotropic displacement coefficients U(H) = 1.2U(C,N) or 1.5U(C_{methyl}), and their coordinates were allowed to ride on their respective atoms. The refinement converged to a final R_1 = 0.1400, and wR_2 = 0.3172 for 9010 reflections of $I > 2\sigma(I)$. Although six noncoordinated lattice solvent sites were identified, the PLATON SQUEEZE calculation for the disordered solvent region (1399.7 Å^3, 43.7% of the crystal volume) showed there are 478 solvent electrons per unit cell, which approximately corresponds to 11.4 CH_2Cl_2 molecules per formula.[12] The structure refinement after modification of the data for the noncoordinated lattice solvent molecules led to better refinement and data convergence. Refinement of the structure converged at a final R_1 = 0.1013, wR_2 = 0.2675 for 7953 reflections with $I > 2\sigma(I)$, R_1 = 0.1190, wR_2 = 0.2784 for all 10770 reflections. The largest difference peak and hole were 1.708 and –1.089 e Å^{-3}, respectively. A summary of the crystal and intensity data is given in Table S1 (Supporting Information).

Crystal Data for $[Mn_6(Haahz)_6(dmf)_2(bpea)_2]$·10dmf (2): $Mn_6C_{114}H_{156}N_{34}O_{24}$, fw = 2716.37 g mol^{-1}, orthorhombic, space group $Pbca$, a = 25.354(5) Å, b = 14.478(3) Å, c = 34.667(7) Å, V = 12725(4) Å^3, Z = 4, μ(synchrotron, λ = 0.70000 Å) = 0.659 mm^{-1}, 70113 reflections were collected, 19104 were unique (R_{int} = 0.0552). The structures was solved by a direct method and refined by full-matrix least-squares calculations with the SHELXTL-PLUS software package. Three manganese atoms, three ligand units, two bpea linkers, one coordinating dmf molecule, and five noncoordinating dmf sites were identified as the asymmetric unit. All non-hydrogen atoms were refined anisotropically; hydrogen atoms bound to the amido nitrogen atom were found in difference Fourier maps and refined with assigned isotropic displacement coefficients U(H) = 1.2U(N), the remaining hydrogen atoms were assigned isotropic displacement coefficients U(H) = 1.2U(C) or 1.5U(C_{methyl}) and their coordinates were allowed to ride on their respective atoms. Some dmf molecules were refined by using disordered models. Refinement of the structure converged at a final R_1 = 0.0473, wR_2 = 0.1269 for 14630 reflections with $I > 2\sigma(I)$, R_1 = 0.0687, wR_2 = 0.1434 for all 19104 reflections. The largest difference peak and hole were 0.860 and –0.816 e Å^{-3}, respectively. A summary of the crystal and intensity data is given in Table S1 (Supporting Information).

CCDC-692747 (for **1**) and -692748 (for **2**) contain the supplementary crystallographic data for this paper. These data can be obtained free of charge from The Cambridge Crystallographic Data Centre via www.ccdc.cam.ac.uk/data_request/cif.

Supporting Information (see footnote on the first page of this article): Additional crystal data and structure refinement for **1** and **2**; space-filling diagrams of network **2**.

Acknowledgments

This work was supported by Hanyang University (2007).

[1] a) J. L. C. Rowsell, E. C. Spencer, J. Eckert, J. A. K. Howard, O. M. Yaghi, *Science* **2005**, *309*, 1350; b) N. L. Rosi, J. Eckert, M. Eddaoudi, D. T. Vodak, J. Kim, M. O'Keeffe, O. M. Yaghi, *Science* **2003**, *300*, 1127; c) X. Zhao, B. Xiao, A. J. Fletcher, K. M. Thomas, D. Bradshaw, M. J. Rosseinsky, *Science* **2004**, *306*, 1012; d) S. M. Kuznicki, V. A. Bell, S. Nair, H. W. Hillhouse, R. M. Jacubinas, C. M. Braunbarth, B. H. Toby, M. Tsapatsis, *Nature* **2001**, *412*, 720; e) S. Ma, D. Sun, X.-S. Wang, H.-C. Zhou, *Angew. Chem.* **2007**, *119*, 2510; *Angew. Chem. Int. Ed.* **2007**, *46*, 2458; f) J. S. Seo, D. Whang, H. Lee, S. I. Jun, J. Oh, Y. J. Jeon, K. Kim, *Nature* **2000**, *404*, 982; g) C.-D. Wu, A. Hu, L. Zhang, W. Lin, *J. Am. Chem. Soc.* **2005**, *127*, 8940.

[2] a) M. Eddaoudi, D. B. Moler, H. Li, B. Chen, T. M. Reineke, M. O'Keeffe, O. M. Yaghi, *Acc. Chem. Res.* **2001**, *34*, 319; b) F. A. Cotton, C. Lin, C. A. Murillo, *Acc. Chem. Res.* **2001**, *34*, 759; c) S. A. Bourne, J. Lu, A. Mondal, B. Moulton, M. J. Zaworotko, *Angew. Chem. Int. Ed.* **2001**, *40*, 2111; d) C. Serre, F. Millange, S. Surblé, G. Férey, *Angew. Chem.* **2004**, *116*, 6445; *Angew. Chem. Int. Ed.* **2004**, *43*, 6285; e) H. K. Chae, D. Y. Siberio-Pérez, J. Kim, Y. Go, M. Eddaoudi, A. J. Matzger, M. O'Keeffe, O. M. Yaghi, *Nature* **2004**, *427*, 523; f) E.-C. Yang, J. Li, B. Ding, Q.-Q. Liang, X.-G. Wang, X.-J. Zhao, *CrystEngComm* **2008**, *10*, 158; g) S. Ma, X.-S. Wang, E. S. Manis, C. D. Collier, H.-C. Zhou, *Inorg. Chem.* **2007**, *46*, 3432; h) A. Thirumurugan, S. Natarajan, *Cryst. Growth Des.* **2006**, *6*, 983.

[3] a) M. Eddaoudi, J. Kim, N. Rosi, D. Vodak, J. Wachter, M. O'Keeffe, O. M. Yaghi, *Science* **2002**, *295*, 469; b) O. M. Yaghi, M. O'Keeffe, N. W. Ockwig, H. K. Chae, M. Eddaoudi, J. Kim, *Nature* **2003**, *423*, 705; c) N. W. Ockwig, O. Delgado-Froedrichs, M. O'Keeffe, O. M. Yaghi, *Acc. Chem. Res.* **2005**, *38*, 176.

[4] a) E. Lee, J. Kim, J. Heo, D. Whang, K. Kim, *Angew. Chem.* **2001**, *113*, 413; *Angew. Chem. Int. Ed.* **2001**, *40*, 399; b) J. J. Bodwin, V. L. Pecoraro, *Inorg. Chem.* **2000**, *39*, 3434; c) V. L. Pecoraro, J. J. Bodwin, A. D. Cutland, *J. Solid State Chem.* **2000**, *152*, 68; d) Y. Zou, M. Park, S. Hong, M. S. Lah, *Chem. Commun.* **2008**, 2340; e) J. J. Perry IV, V. C. Kravtsov, G. J. McManus, M. J. Zaworotko, *J. Am. Chem. Soc.* **2007**, *129*, 10076; f) A. J. Cairns, J. A. Perman, L. Wojtas, V. C. Kravtsov, M. H. Alkordi, M. Eddaoudi, M. Zaworotko, *J. Am. Chem. Soc.* **2008**, *130*, 1560; g) R. Wang, M. Hong, J. Luo, R. Cao, J. Weng, *Chem. Commun.* **2003**, 1018; h) J. Park, S. Hong, D. Moon, M. Park, K. Lee, S. Kang, Y. Zou, R. P. John, G. H. Kim, M. S. Lah, *Inorg. Chem.* **2007**, *46*, 10208.

[5] a) B. Kwak, H. Rhee, M. S. Lah, *Inorg. Chem.* **1998**, *37*, 3599; b) B. Kwak, H. Rhee, M. S. Lah, *Polyhedron* **2000**, *19*, 1985.

[6] a) M. Moon, I. Kim, M. S. Lah, *Inorg. Chem.* **2000**, *39*, 2710; b) D. Moon, J. Song, B. J. Kim, B. J. Suh, M. S. Lah, *Inorg. Chem.* **2004**, *43*, 8230; c) D. Moon, M. S. Lah, *Inorg. Chem.* **2005**, *44*, 1934; d) R. P. John, D. Moon, M. S. Lah, *Supramol. Chem.* **2007**, *19*, 295.

[7] a) S. Lin, S.-X. Liu, Z. Chen, B.-Z. Lin, S. Gao, *Inorg. Chem.* **2004**, *43*, 2222; b) S. Lin, S.-X. Liu, J.-Q. Huang, C.-C. Lin, *J. Chem. Soc., Dalton Trans.* **2002**, 1595; c) R. P. John, K. Lee, B. J. Kim, B. J. Suh, H. Rhee, M. S. Lah, *Inorg. Chem.* **2005**, *44*, 7109; d) S.-X. Liu, S. Lin, B.-Z. Lin, C.-C. Lin, J.-Q. Huang, *Angew. Chem.* **2001**, *113*, 1118; *Angew. Chem. Int. Ed.* **2001**, *40*, 1084; e) R. P. John, K. Lee, M. S. Lah, *Chem. Commun.* **2004**, 2660; f) R. P. John, J. Park, D. Moon, K. Lee, M. S. Lah, *Chem. Commun.* **2006**, 3699; g) R. P. John, M. Park, D. Moon, K. Lee, S. Hong, Y. Zou, C. S. Hong, M. S. Lah, *J. Am. Chem. Soc.* **2007**, *129*, 14142; h) K. Lee, R. P. John, M. Park, D. Moon, H.-C. Ri, G. H. Kim, M. S. Lah, *Dalton Trans.* **2008**, 131; i) D. Moon, K. Lee, R. P. John, G. H. Kim, B. J. Suh, M. S. Lah, *Inorg. Chem.* **2006**, *45*, 7991.

[8] M. Park, R. P. John, D. Moon, K. Lee, G. H. Kim, M. S. Lah, *Dalton Trans.* **2007**, 5412.

[9] R. Wang, D. Yuan, F. Jiang, L. Han, S. Gao, M. Hong, *Eur. J. Inorg. Chem.* **2006**, 1649.

[10] C. S. Alvarez, A. D. Bond, D. Cave, M. E. G. Mosquera, E. A. Harron, R. A. Layfield, M. McPartlin, J. M. Rawson, P. T. Wood, D. S. Wright, *Chem. Commun.* **2002**, 2980.

[11] a) M. O'Keeffe, S. T. Hyde, *Zeolites* **1997**, *19*, 370; b) G. O. Brunner, *Zeolites* **1993**, *13*, 592.

[12] PLATON program: A. L. Spek, *Acta Crystallogr., Sect. A* **1990**, *46*, 194.

[13] *SMART and SAINT, Area Detector Software Package and SAX Area Detector Integration Program*, Bruker Analytical X-ray, Madison, WI, **1997**.

[14] *SADABS, Area Detector Absorption Correction Program*, Bruker Analytical X-ray, Madison, WI, **1997**.

[15] A. J. Arvai, C. Nielsen, *ADSC Quantum-210 ADX Program*, Area Detector System Corporation, Poway, CA, USA, **1983**.

[16] Z. Otwinowski, W. Minor in *Methods in Enzymology*, (Eds.: C. W. Carter Jr., R. M. Sweet), Academic Press, New York, **1997**, vol. 276, part A, p. 307.

[17] G. M. Sheldrick *SHELXTL–PLUS*, *Crystal Structure Analysis Package*, Bruker Analytical X-ray, Madison, WI, **1997**.

Received: July 3, 2008
Published Online: November 4, 2008

